Energy Conversion and Management 120 (2016) 44–50

Contents lists available at ScienceDirect

Energy Conversion and Management

journal homepage: www.elsevier.com/locate/enconman

Effect of changing the water balance on electro-osmotic flow in an elliptical single proton exchange membrane fuel cell

Mohammad Gholizadeh [a], Mohsen Ghazikhani [a], Iman Khazaee [b,*]

[a] Department of Mechanical Engineering, Ferdowsi University, Mashhad, Iran
[b] Department of Mechanical and Energy Engineering, Shahid Beheshti University, A.C., Tehran, Iran

ARTICLE INFO

Article history:
Received 17 February 2016
Received in revised form 23 April 2016
Accepted 25 April 2016

Keywords:
Fuel cell
Electro osmotic
Elliptical
Humidity
Back diffusion

ABSTRACT

In this study, the effect of water balance variation on electro-osmotic flow in a fuel cell with elliptical cross section has been investigated experimentally. By changing the humidity on both sides of the fuel cell, required data for electro-osmotic flow and back diffusion were calculated. In addition, using the balance equations for water's mass at anode and cathode, the values of the electro-osmotic flow and back diffusion in different current densities were found. Results show that variations of the electro-osmotic flow and back diffusion change linearly with current density and slope of the curves increase by increasing in humidity. Besides, after a certain value, humidity raise has a negligible effect on curves of electro-osmotic flow and back diffusion. In other words, there is an optimum value for humidity at anode and cathode side. Based on the results, it was determined that increasing in humidity at anode side has a more desirable effect than the cathode. For instance, when cathode and anode had the humidity level of 0% and 70% respectively, maximum current density of the fuel cell was recorded about 0.86 A/cm^2 but when cathode and anode had the humidity level of 70% and 0% respectively, maximum current density of the fuel cell was obtained about 0.512 A/cm^2. Using available equations, electro-osmotic coefficients were also calculated and their variations with respect to current density and humidity level were outlined. Results show that electro-osmotic coefficient remains constant with respect to current density, while it increases with increasing the humidity. In this work, electro-osmotic coefficients varied between 0.636001 and 1.632476, which were in a good agreement with the values in other related papers.

1. Introduction

Since the world's energy resources and reserves are limited, humans look everyday for ways to maximize the efficient use of available energy resources. One of the energy converters in which the chemical energy of fuel converts to electric energy is the fuel cell. It, with no long history, has received much attention by researchers and scientists in recent decades. There are different kinds of fuel cells that can be used in various operating and environmental conditions as Proton Exchange Membrane Fuel Cell (PEMFC) is one of them.

One of the issues of particular importance in the PEM fuel cell is the wettability of membrane. Wettability of membrane increases proton conductivity from the anode to the cathode and loss of water makes proton conductivity difficult. In the PEM fuel cell membrane, the proton, moving from the anode to the cathode, transfers water molecules with it, so the anode water decreases as a result. Loss in anode water and consequently, the increase in the cathode water impairs the fuel cell performance and results in a drop in the efficiency. Checking the water content in various parts of the fuel cell is an important issue on which various researches, tests and modeling. Clearly, there are no sufficient researches and tests in this area and certainly, more research is needed in this regard.

Karimi and Li [1] modeled the electro-osmotic flow in the polymer membrane along with electro-kinetic effect, and determined the key parameters affecting the PEM fuel cell performance. Mulyazmi et al. [2] investigated the water balance in a PEM fuel cell based on the water transport phenomena. In this investigation, the diffusion of water from the cathode side to the anode side of the cell was observed to not occur at 20% relative humidity at the cathode and 58% relative humidity at the anode. Yan et al. [3] examined the water balance in the PEM fuel cell measuring the net drag coefficients under different conditions. They also studied the effects of water balance in the membrane on the fuel cell

* Corresponding author.
E-mail addresses: i_khazaei@sbu.ac.ir, imankhazaee@yahoo.com (I. Khazaee).

http://dx.doi.org/10.1016/j.enconman.2016.04.094
0196-8904/

performance under various operating conditions. Luo et al. [4] presented a new method based on hydrogen pump to measure the electro-osmotic drag coefficient and proton conductivity in Nafion 117 membrane under similar condition to operating PEM fuel cell. Zhang et al. [5] investigated the transport of water vapor from the cathode to the anode and the effect of water vapor on the performance of a single cell high temperature PEM fuel cell using a commercial PBI-based membrane electrode assembly (MEA). Rakhshanpouri and Rowshanzamir, a seven-layer theoretical model proposed that included anode and cathode inlet channels, GDLs, CLs, and the Nafion 117 proton exchange membrane. The mathematical model was a one-dimensional, steady-state, isothermal and isobar to describe the water transport phenomena in PEM fuel cell [6]. Zhou et al. [7] studied the effects of pressure and water on a single PEM fuel cell. Karpenko-Jereb et al. presented the development of a 1D model describing water and charge transport through the polymer electrolyte membrane in the fuel cell. The dependencies of diffusion and electro-osmotic coefficients on the membrane water concentration described by linear functions [8]. Tiss et al. [9] developed a two-dimensional computational fluid dynamics model of PEM fuel cell by taking into account the electrochemical, mass and heat transfer process occurring in the cathode compartment. This model included the effect of water content in the membrane swelling phenomenon. Zhang et al. [10] analyzed the water balance within a PEM fuel cell, and introduced multiple equations as the functions of input and output pressures of the fuel cell gas flow, the input relative humidity, temperature, pressure losses across the flow channels and the partial pressure of the reactants. Bezmalinović et al. carried out a study of water transport in a high temperature phosphoric acid doped polybenzimidazole (PBI) membrane fuel cell stack. Tests with different stoichiometries of dry cathode and different humidity levels of anode are performed. The water transport was a strong function of current density but it also depended on stoichiometry and humidity level [11]. Perng et al. [12] investigated how modified flow field affected non-isothermal transport characteristics and performance of the PEM fuel cell by the finite-volume SIMPLEC method coupled with preconditioned conjugate gradient methods. The results demonstrated that the narrowed flow channel with ribs opposite the protuberant catalyst layer surface had the best increase rate in cell performance. Husar et al. [13] measured water transport in situ through the membrane regarding the separate mechanisms in a PEM fuel cell. Park and Caton using water balance tests, obtained electro-osmotic drag coefficients (n_d) in Nafion 115 membrane under different conditions as a function of humidity and thermodynamic conditions [14]. Park investigated the effect of polytetrafluoroethylene coated gas diffusion medium on the water content in the membrane electrolyte. Numerical simulation suggested that the optimum water saturation was between 0.1 and 0.3 at the gas diffusion medium to hydrate the membrane electrolyte sufficiently without significantly blocking the diffused species under non-humidification conditions [15]. Cha et al. [16] the effects of the clamping force on the water transport and performance characteristics of a PEM fuel cell experimentally investigated with variations in the relative humidity and current density. The water transport characteristics were analyzed by calculating the net drag coefficient. Dai et al. reviewed the experimental studies and modeling works on the water transport and balance in various components of MEA [17]. Li et al. [18] reported the preparation and characterization of porous polybenzimidazole membranes doped with phosphoric acid. In addition, they tested the performance and stability of the porous PBI membrane in high-temperature proton-exchange-membrane fuel cells. Liso et al., a novel mathematical zero-dimensional model formulated for the water mass balance and hydration of a polymer electrolyte membrane. This model incorporated all the essential fundamental physical and electrochemical processes occurring in the membrane electrolyte and considered the water adsorption/desorption phenomena in the membrane [19]. Saeed et al. [20] studied several variables in order to evaluate the performance of PEM fuel cell with an active area of 25 cm^2. Also, they added SiO_2 particles to the Nafion polymeric matrix using sol–gel method in order to increase the performance of membrane. Das et al. [21] for investigating the water transport in the cathode catalyst layer (CCL) of a PEM fuel cell performed a one-dimensional analytical solution of water transport across the CCL using the fundamental transport equations. Hsieh et al. [22] conducted time-dependent measurements of pressure drop in different flow fields on the cathode of a PEM fuel cell with different flow rates and temperatures on current distribution. In addition, they investigated the effects of pressure drop, flow rates and cell temperature on water accumulation. Bao and Bessler developed a two-dimensional single-phase model for the steady-state and transient analysis of polymer electrolyte membrane fuel cells. They used the model to analyze the effects of operating conditions on current output and water management, especially net water transport coefficient along the channel [23]. Mahmoudi et al. [24] investigated numerically the effects of inhomogeneous compression of GDL at the cathode side of PEM fuel cell with interdigitated flow field on water management and cell performance. Jeon et al. studied the effect of cathode relative humidity on the PEM fuel cell focusing on its self-developing function [25]. Misran et al. [26] have experimentally investigated the effect of the water content within the PEM fuel cell membrane in the dry and humidity 100% states at different temperatures by electro-osmotic drag coefficient, back diffusion coefficient.

In this paper, we focused specifically on electro-osmotic coefficient and the level of its changes was obtained by the change in water balance and the empirical relationships. Also the relationships related to the water mass balance were analyzed. In this research experimental setup, the water balance change was created by changing humidity in the anode and cathode inlet gases and the humidity changed between dry and 100% states. By changing the humidity and recording the data of different parts of the fuel cell and using the existing empirical and thermodynamic equations, electro-osmotic drag coefficients were calculated and analyzed at different states. It should be noted that besides electro-osmotic flow, back diffusion flow was also studied due to its relationship with the water balance in the membrane.

2. Experimental setup

The dimension of mentioned fuel cell is 4.5 cm × 9.5 cm × 10.1 cm. The MEA is constructed using catalytic-coated membrane method [27,28]. Nafion ionomer is used as a proton conducting membrane in the MEA and the loading of Pt electrocatalyst (IERC Research Center, M. Nasr) on both anode and cathode is 4 mg/cm^2 [29]. Also, the gas diffusion layers on both sides of proton exchange membrane are made of carbon clothes and the bipolar plates as a conductor of electric current are made of graphic. The stainless steel plates are used to maintain the MEA. In addition, the channels are in form of four serpentine flow fields with an elliptical cross-section. The dimensional characteristics of single PEM fuel cell are shown in Table 1.

To achieve the required data, in addition to the single fuel cell, equipments such as rotameter, pressure gauge, humidifier, thermometer, condenser, gas capsule and digital scale were also needed that were all used in a workbench. Fig. 1 shows a schematic of the experimental setup.

In this work, the oxygen was used instead of air on the cathode side. The pressure of hydrogen and oxygen were considered 2 bar in all tests and the fuel cell temperature was also considered

Table 1
Dimensional characteristics of single four-channel PEM fuel cell.

Description	Unit	Value
Active area	cm^2	25
Catalyst layer thickness	cm	0.001
Gas diffusion layer thickness	cm	0.033
Bipolar plate thickness	cm	0.5
Channel length	cm	4.8
Distance between each channel	cm	0.1
Stainless steel plates thickness	cm	2

55 °C in all tests. Also, the relative humidity of inlet gases on both the anode and cathode sides was changed from zero to 100% using bubbling technique, and the gas flow rate entering the fuel cell was also measured. A condenser, thermometer, rotameter and psychrometer were used in the anode and cathode outputs of fuel cell, respectively, which recorded the required data. In all mathematical calculations related to the electro-osmotic flow discussed in Section 4, hydrogen and oxygen were assumed as ideal gas. Obviously, three factors of electro-osmosis, back diffusion and convection play the main roles in the water balance of a PEM fuel cell. In this study, the convection effect was ignored due to the fact that the pressure on both sides of anode and cathode are equal.

To record current and voltage of fuel cell, an electrical load source (Electrical Load Bank), working at 0–35 A, was applied. A switch on the ELB was turned to read voltage and current values and then current passed the cell fuel increased and voltage decreased. The current grew consistently too slightly by turning the switch and then fixed although the voltage of the fuel cell declined. On the other hand, there is a maximum value of the output current in a test which can be obtained by this approach.

3. Electro-osmotic phenomenon

Electro-osmotic flow in a solution is caused by the Coulomb force induced by an electric field on mobile electric charge near the surface. The chemical equilibrium between a solid surface and an electrolyte solution results in the interface acquiring a net fixed electrical charge, therefore, layers of oppositely charged ions (known as an electrical double layer) form in the region near the interface between the solution and the wall. When an electric field is applied to the fluid, ions are forced to move by the resulting Coulomb force in the mobile layer. The resulting flow is known as electro-osmotic flow [30–32].

Electro-osmotic flow is shown in Fig. 2. The solid surface is exposed to an electrolyte solution and obtains negative charge. This charge created on the surface absorbs the oppositely charged ions scattered in the solution, and a thin layer of positive ions is formed near the walls of the channel where the concentration of positive ions is locally more than other parts of the solution. When an electric field is applied to the solution, this layer, consisting of positive ions, moves toward the negative electrode (cathode) and moves the fluid bulk to the negative electrode as well [33].

In the PEM fuel cell, electro-osmotic flow caused water molecules move from the anode side (positive pole) to the cathode side (negative pole). This process results in water loss at the anode side and water increase in the cathode side. Of course, a flow called water back diffusion caused by the increased water concentration in the cathode side opposes electro-osmotic flow. The balance between these two phenomena would make the fuel cell function properly.

4. Calculation of water balance in the membrane

To examine the water balance in a PEM fuel cell, some mathematical equations are needed. Water balance equation by the molar flow rate in the PEM fuel cell can be written on the cathode and anode sides as following:

$$Anode: \quad \dot{N}^{out}_{v,a} + \dot{N}_{Condense,a} = \dot{N}^{in}_{v,a} - \dot{N}^{EOF}_{v} + \dot{N}^{B.D.}_{v} \tag{1}$$

$$Cathode: \quad \dot{N}^{out}_{v,c} + \dot{N}_{Condense,c} = \dot{N}^{in}_{v,c} + \dot{N}^{P}_{v} + \dot{N}^{EOF}_{v} - \dot{N}^{B.D.}_{v} \tag{2}$$

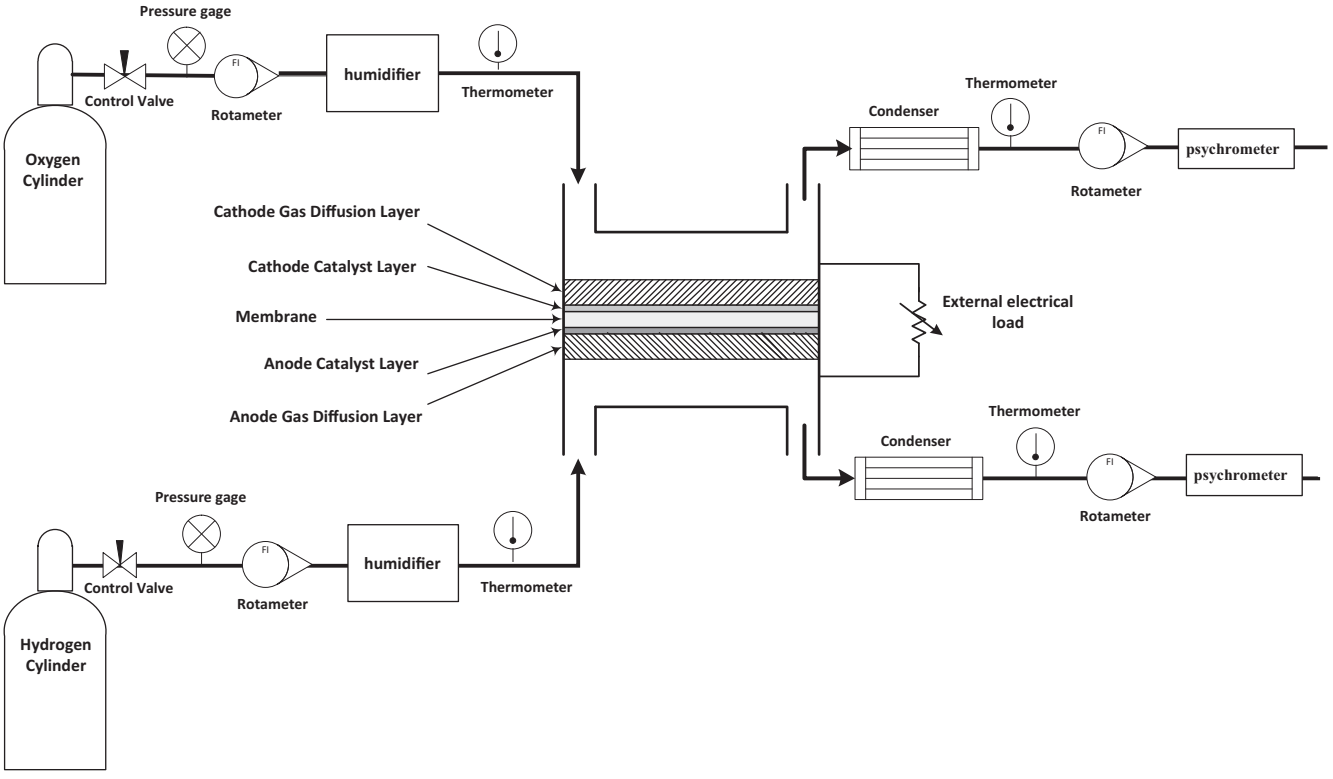

Fig. 1. Schematic illustration of the experimental setup.

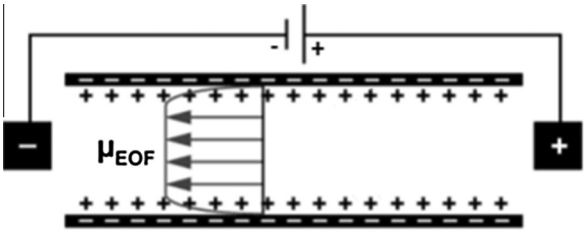

Fig. 2. Electro-osmotic flow in a micro-channel.

In this equations, $\dot{N}^{in}_{v,a}$ and $\dot{N}^{in}_{v,c}$ are the molar flow rates of inlet water vapor in the anode and cathode, respectively. Also, $\dot{N}^{out}_{v,a}$ and $\dot{N}^{out}_{v,c}$ are the molar flow rates of outlet water vapor in the anode and cathode, respectively, whose values are calculated by the following ideal gas equation:

$$\dot{N}^{=}_{v}\frac{P_v\dot{V}}{\bar{R}T} \tag{3}$$

where P_v, $\dot{V}$ and T are the partial pressure of water vapor, volumetric flow rate and temperature of the mixture, respectively. P_v can be calculated by the following equation [10]:

$$P_v = \emptyset \times P_{sat|T} \tag{4}$$

where $\emptyset$ and $P_{sat|T}$ are the relative humidity and saturation vapor pressure at the desired temperature, respectively. The value of $P_{sat|T}$ can be obtained by the following equation [10]:

$$\begin{aligned} P_{sat|T} &= 6.02724\times10^{(-3)} + 4.38484\times10^{(-4)} * T \\ &\quad + 1.39844\times10^{(-5)} * T^2 + 2.71166\times10^{(-7)} * T^3 \\ &\quad + 2.57731\times10^{(-9)} * T^4 + 2.82254\times10^{(-11)} * T^5 \end{aligned} \tag{5}$$

where T and $P_{sat|T}$ are in degrees Celsius and atm, respectively.

In Eqs. (1) and (2), the expression $\dot{N}_{Condense}$ represents the molar flow rate of condensed water in the outlet gases of the fuel cell stored in a dehumidifier and determined by the digital scale. Also, in the mentioned equations, $\dot{N}^{P}_{v}$ and $\dot{N}^{EOF}_{v}$ are the molar flow rate of water produced at the cathode side and the molar flow rate of electro-osmotic flow, respectively, whose values are obtained by the following equations [7,34]:

$$\dot{N}^{P}_{v} = \frac{I}{2F} \tag{6}$$

$$\dot{N}^{EOF}_{v} = n_d\frac{I}{F} \tag{7}$$

where I represents the current density of fuel cell, F is the Faraday number whose value equals to 96,487 C/mol and n_d is the electro-osmotic coefficient where is evaluated as [34]:

$$n_d = \begin{cases} 0.0049 + 2.02a - 4.53a^2 + 4.09a^3 & : \ 0 < a \leqslant 1 \\ 1.5849 + 0.159(a-1) & : \ a > 1 \end{cases} \tag{8}$$

In this equation, a is the activity of water vapor in the membrane whose value can be obtained by the following equation [34]:

$$a_j = y_i\frac{P_j}{P_{sat,j}} \tag{9}$$

where y_i is the mole fraction of water vapor in the mixture and the index j represents the anode or cathode.

Given that the activity of water vapor in the membrane results from the activity of water vapor in the anode and cathode, so the activity of water vapor in membrane can be estimated as the average of these values using the activity of water vapor in the anode and cathode, then we have [2]:

$$a = \frac{a_{anode} + a_{cathode}}{2} \tag{10}$$

In this paper, the activity of water vapor in the anode side and cathode was considered as the mean value of the inlet and outlet flows. With values of different expressions in Eqs. (1) or (2), the molar flow rate of back diffusion ($\dot{N}^{B.D.}_{v}$) can be calculated.

According to the experimental data for each current density, electro-osmotic coefficient and back diffusion were obtained and their diagram was drawn and analyzed in each test by current density. Since the number of test cases was high, then experimental data were presented in Table 2 for a specific state. According to Table 2, there is very little difference between the values of back diffusion and net drag obtained from Eqs. (1) and (2). Admittedly, there are some errors in the every experimental study, so it is normal to see some differences in the results. In this work, the mean values of data are used for plotting the graph of back diffusion and net drag.

5. Results and discussion

5.1. The effect of humidity change on electro-osmotic flow

5.1.1. Humidity change in cathode side

The effect of humidity change on the anode side and cathode side has discussed in this section. Considering the anode humidity 70% and the cathode humidity change between 0%, 35%, 70% and 100%, the experimental data were recorded. For the experimental data at different current densities, electro-osmotic flow and its coefficients were calculated in each experiment and their diagram was drawn as shown in Figs. 3 and 4 for electro-osmotic flow and electro-osmotic coefficient, respectively. In these experiments, the volumetric flow rate of anode and cathode gases was considered 8.3333 cm^3/s (0.5 L/min).

As seen in Fig. 3, electro-osmotic flow increases almost linearly with current density. It is clear that based on this figure, with increasing cathode humidity, the diagram slope increases. In fact, the more humidity increases in the cathode side, the slope of electro-osmotic flow increases by current density, and the easier electro-osmotic flow is created. Since the cathode humidity increases, the humidity in the membrane increases, therefore, it is logical that the value of the electro-osmotic flow, directly related to the humidity in the membrane, increased as well.

Fig. 4 shows the variations of electro-osmotic coefficient in different current densities. According to the figure, at lower cathode humidity, as the current density increases, electro-osmotic coefficient is reduced and gradually reaches to a steady state. As the cathode humidity increases, small changes seen at low humidity

Table 2
The obtained values from Eqs. (1) and (2) in special state (RHC = 100%, RHA = 70%).

Expression (mol/cm^2 s)	I = 0.2 (A/cm^2)	I = 0.6 (A/cm^2)	I = 1 (A/cm^2)
$\dot{N}^{in}_{v,Anode}$	8.452E−07	8.452E−07	8.452E−07
$\dot{N}^{out}_{v,Anode}$	7.218E−07	1.632E−06	2.647E−06
$\dot{N}^{in}_{v,Cathode}$	1.207E−06	1.207E−06	1.207E−06
$\dot{N}^{out}_{v,Cathode}$	7.782E−07	1.594E−06	2.586E−06
$\dot{N}_{Cond.Anode}$	2.963E−07	3.333E−07	5.185E−07
$\dot{N}_{Cond.Cathode}$	1.296E−06	1.407E−06	1.63E−06
$\dot{N}^{P}_{v}$	1.036E−06	3.109E−06	5.182E−06
$\dot{N}_{EOF}$	3.347E−06	1.003E−05	1.672E−05
$\dot{N}^{Net\text{-}Drag}_{Cathode}$	−1.69E−07	−1.32E−06	−2.174E−06
$\dot{N}^{Net\text{-}Drag}_{Anode}$	−1.73E−07	−1.12E−06	−2.321E−06
$\dot{N}^{B.D.}_{Cathode}$	3.516E−06	1.135E−05	1.89E−05
$\dot{N}^{B.D.}_{Anode}$	3.52E−06	1.115E−05	1.904E−05

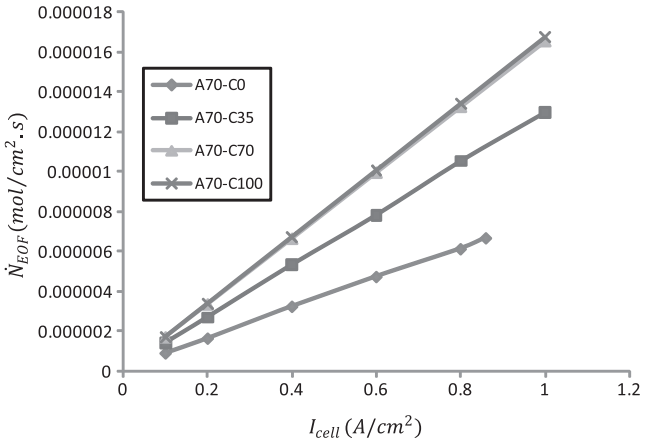

Fig. 3. Variations of electro-osmotic flow versus current density at different cathode humidity levels.

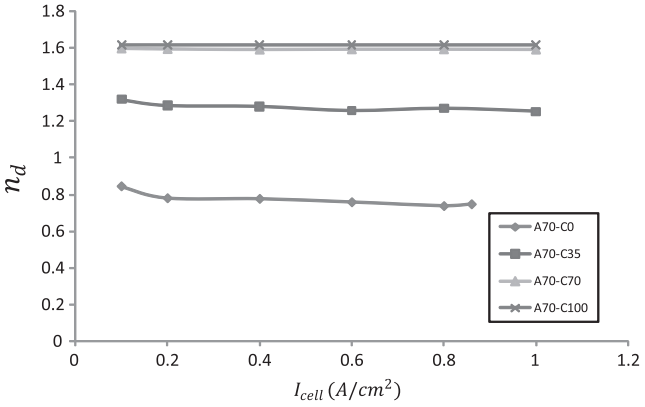

Fig. 4. Variations of electro-osmotic coefficient (n_d) with current density at different cathode humidity levels.

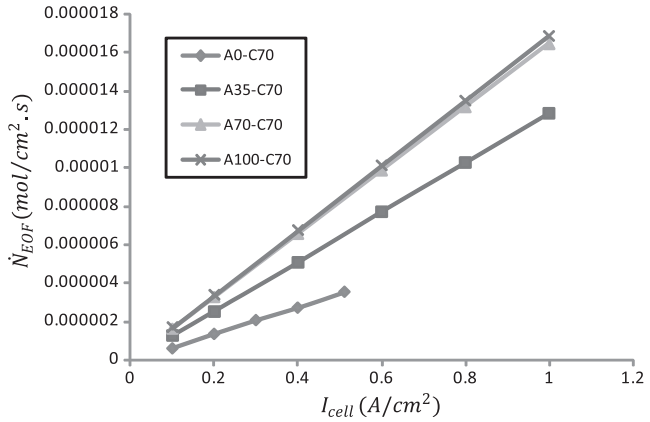

Fig. 5. Variations of electro-osmotic flow with current density at different anode humidity levels.

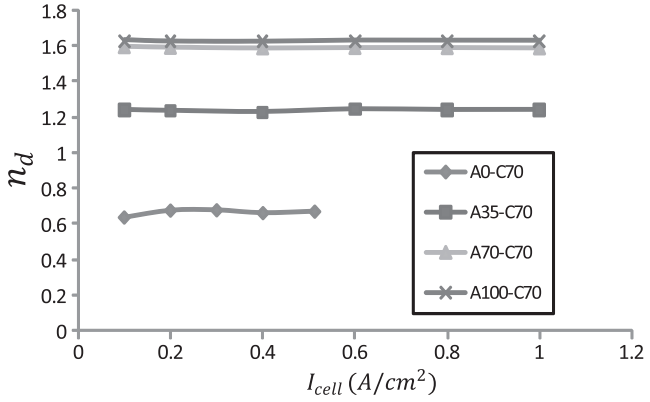

Fig. 6. Variations of electro-osmotic coefficient with current density at different anode humidity levels.

levels and electro-osmotic coefficient remains almost constant in different current densities. The reason might be that increasing the current density, leads to increasing the movement of protons from the anode side to the cathode side and leads to increasing the produced water in the cathode side. We know that the water produced at the cathode results in the back flow of water to the anode, and this is against the water flow of protons running from the anode to the cathode, therefore, a balance state is created in electro-osmotic drag coefficient. It is clear that the optimum humidity would be between 70% and 100% according to the results.

5.1.2. Humidity change in anode side

After analyzing the effect of cathode humidity change on electro-osmotic flow, the effect of anode humidity change was studied. In this case, considering the cathode humidity 70% and the anode humidity changes between 0%, 35%, 70% and 100%, tests were carried out and the resulting diagrams were analyzed using the experimental data. After the calculation, the diagram of electro-osmotic flow changes at the anode different humidity levels was drawn by current density in Fig. 5.

The variations of electro-osmotic flow in Fig. 5 were similar to Fig. 3. In other words, Fig. 5 shows that the humidity change in the anode side and cathode side creates similar effects on electro-osmotic flow, and perhaps the only difference between these two figures is their values. For example, at zero anode humidity and cathode humidity of 70% and the current density of 0.4 A/cm^2, the value of electro-osmotic flow was 2.739E−06 mol/s cm^2, while at zero cathode humidity and anode humidity of 70% with the same current density, this value was 3.222E−06 mol/s cm^2. In general, based on the values obtained, electro-osmotic flow shows larger values at higher anode humidity. It is clear that the optimum humidity would be between 70% and 100% according to the results.

Fig. 6 shows electro-osmotic coefficients with current density at anode different humidity levels. In this figure, similar to Fig. 4, electro-osmotic coefficients are almost constant and only increases with the increasing humidity. Due to the dependency of this coefficient on the water activity in the membrane, it was expected that its diagrams in the anode and cathode are similar except of a slightly difference. Since the activity of water in the membrane is approximated as the mean value of anode and cathode humidity, and inlet humidity levels are equal as shown in Figs. 4 and 6, therefore, the diagrams must be analogous approximately.

5.2. The effect of humidity change on net drag flow

5.2.1. Humidity change in cathode side

According to Fig. 7, it is clear that as the cathode humidity increases, the net drag decreases. In fact, by increasing the cathode humidity, water back diffusion increased and this reduced the amount of net drag which is the difference between water back diffusion and electro-osmotic flow. However, as seen in Fig. 7, there is almost very little difference between the diagrams at high humidity levels, and this might reflect the fact that there is an optimized state in humidification of the cathode side.

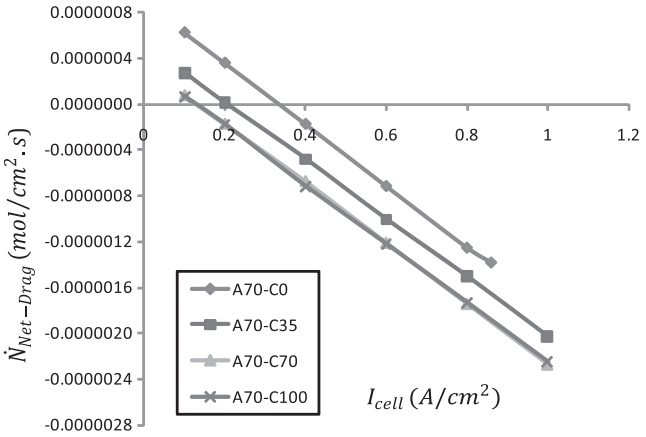

Fig. 7. Variations of net drag with current density at different cathode humidity levels.

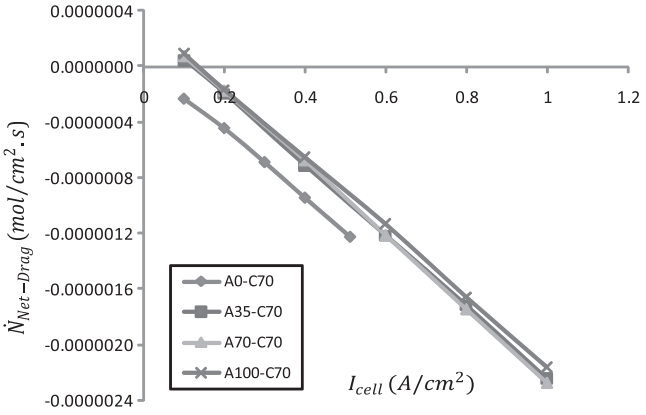

Fig. 8. Variations of net drag with current density at different anode humidity levels.

5.2.2. Humidity change in anode side

According to Fig. 8, it could be said that in this state, unlike the previous state, increasing the anode humidity results increasing the net drag. In fact, with increasing the anode humidity, electro-osmotic flow is reinforced and net drag, as the difference between the back diffusion and electro-osmotic flow, increases as well. In this state, similar to Fig. 7, as humidity increases, diagrams undergo fewer changes and become more similar, and an optimal state can be achieved.

5.3. The effect of humidity change on back diffusion

5.3.1. Humidity change in cathode side

As shown in Fig. 9, changing the cathode humidity increases the water back diffusion from the cathode side to the anode side. Diagrams indicate that back diffusion flow varies almost linearly by current density and the slope of the lines increases at higher humidity levels. Also, it is seen that the cathode humidity levels of 70% and 100% have almost similar diagrams and not much difference is seen between them. This point, like in the previous figures, shows an optimal state in humidification of the fuel cell.

5.3.2. Humidity change in anode side

Looking at Fig. 10, it is found that increasing the anode humidity has an effect similar to that of the increasing cathode humidity on the back diffusion. In fact, increasing the anode humidity also increases the back diffusion, and its difference with the previous

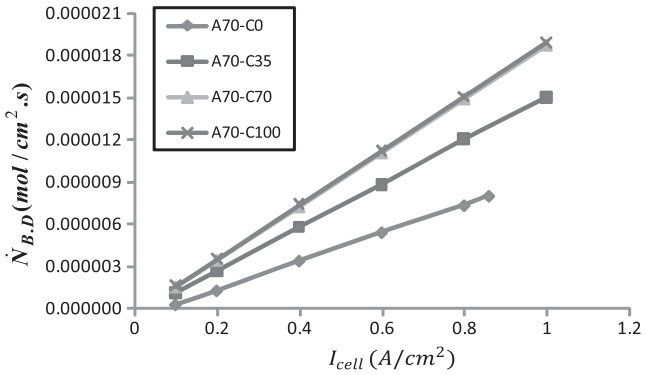

Fig. 9. Variations of back diffusion flow with current density at different cathode humidity levels.

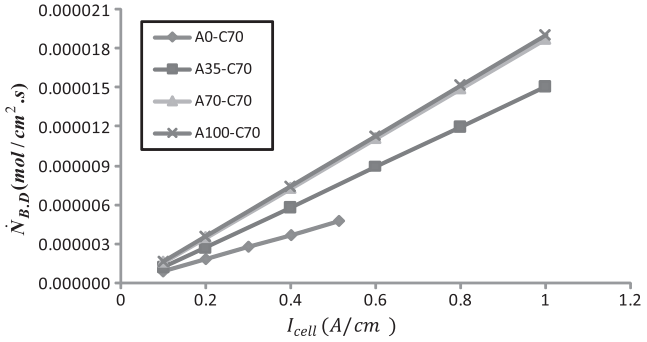

Fig. 10. Variations of back diffusion flow with current density at different anode humidity levels.

Table 3
The comparison of electro-osmotic coefficients in this study and other researchers.

Researchers	Experimental condition	Electro-osmotic coefficient
Yan et al. [3]	T = 80 °C, RHC = 10–100%, RHA = 0–100%	1.66–2
Park and Caton [14]	T = 70 °C, RHC = 0, RHA = 100%	0.5–0.82
Husar et al. [13]	T = 60 °C, RHC = 100%, RHA = 100%	0.65–1.03
Present study	T = 55 °C, RHC = 0–100%, RHA = 0–100%	0.64–1.63

state relates to the diagrams slope and its values. When the cathode humidity is 70%, it might be expected that the values of the back diffusion diagram be decreased as the anode humidity increases, but this expectation would not be realized. Increasing the anode humidity leads to increasing the water activity in the membrane and reinforces electro-osmotic flow. Increasing the electro-osmotic flow increases water accumulation in the cathode side, and back diffusion flow would be reinforced, so back diffusion would be greater at higher anode humidity levels.

At the end, the electro-osmosis coefficients obtained in the present study were compared with other researchers' achievements in Table 3. As shown in Table 3, the range of electro-osmotic coefficient variation is different in various experiments. Since every test has specific condition and the experimental method of every researcher is distinguish, then a specific value of electro-osmotic coefficient cannot be clarified. According to the results obtained by others, it can be concluded that the electro-osmotic coefficients vary in a known range. This range obtained in the present study is 0.64–1.63 which the values of electro-osmotic coefficients presented in Table 3 confirm it.

6. Conclusion

In this study, the water balance in the membrane of a single cell PEM fuel cell with an elliptical cross-section was experimentally carried out. Given to the results, it was found that electro-osmotic flow changes almost linearly by current density. In addition, the results revealed that the variations occur rarely from certain humidity and therefore, an optimal humidity for the anode and cathode can be achieved. However, there was a difference between the cathode and anode diagrams and the electro-osmotic flow was higher whereas the anode humidity was increased more. The electro-osmotic coefficient value was almost constant with current density at any humidity level, and some increase in electro-osmotic coefficient was only seen in low current densities and lower humidity levels. Studying the variations of back diffusion flow, it was seen that the amount of this parameter increased with the increasing anode and cathode humidity. Back diffusion flow diagrams were almost linear and their slope increased with the increasing anode or cathode humidity. According to the experimental data and drawn diagrams, it was seen that as the cathode humidity increased, the back diffusion also increases. One of the interesting points, in addition to the above results, was that at zero cathode humidity and anode humidity of 70%, the maximum current density of fuel cell was recorded 0.86 A/cm^2, whereas this value was 0.512 A/cm^2 at zero anode humidity and cathode humidity of 70%. Considering this point, it could be said that humidification has a great importance on both sides of the fuel cell, but humidification in the anode side has more important than in the cathode side, for increasing the cell efficiency.

References

[1] Karimi G, Li X. Electroosmotic flow through polymer electrolyte membranes in PEM fuel cells. J Power Sources 2005;140:1–11.
[2] Mulyazmi N, Daud W, Majlan E, Rosli M. Water balance for the design of a PEM fuel cell system. Int J Hydrogen Energy 2013;38:9409–20.
[3] Yan Q, Toghiani H, Wu J. Investigation of water transport through membrane in a PEM fuel cell by water balance experiments. J Power Sources 2006;158:316–25.
[4] Luo Z, Chang Z, Zhang Y, Liu Z, Li J. Electro-osmotic drag coefficient and proton conductivity in Nafion® membrane for PEMFC. Int J Hydrogen Energy 2010;35:3120–4.
[5] Zhang C, Zhang L, Zhou W, Wang Y, Chan SH. Investigation of water transport and its effect on performance of high-temperature PEM fuel cells. Electrochim Acta 2014;149:271–7.
[6] Rakhshanpouri S, Rowshanzamir S. Water transport through a PEM (proton exchange membrane) fuel cell in a seven-layer model. Energy 2013;50:220–31.
[7] Zhou B, Huang W, Zong Y, Sobiesiak A. Water and pressure effects on a single PEM fuel cell. J Power Sources 2006;155:190–202.
[8] Karpenko-Jereb L, Innerwinkler P, Kelterer AM, Sternig C, Fink C, Prenninger P, et al. A novel membrane transport model for polymer electrolyte fuel cell simulations. Int J Hydrogen Energy 2014;39:7077–88.
[9] Tiss F, Chouikh R, Guizani A. A numerical investigation of the effects of membrane swelling in polymer electrolyte fuel cells. Energy Convers Manage 2013;67:318–24.
[10] Zhang J, Tang Y, Song C, Xia Z, Li H, Wang H, et al. PEM fuel cell relative humidity (RH) and its effect on performance at high temperatures. Electrochim Acta 2008;53:5315–21.
[11] Bezmalinović D, Strahl S, Roda V, Husar A. Water transport study in a high temperature proton exchange membrane fuel cell stack. Int J Hydrogen Energy 2014;39:10627–40.
[12] Perng SW, Wu HW, Wang RH. Effect of modified flow field on non-isothermal transport characteristics and cell performance of a PEMFC. Energy Convers Manage 2014;80:87–96.
[13] Husar A, Higier A, Liu H. In situ measurements of water transfer due to different mechanisms in a proton exchange membrane fuel cell. J Power Sources 2008;183:240–6.
[14] Park YH, Caton JA. An experimental investigation of electro-osmotic drag coefficients in a polymer electrolyte membrane fuel cell. Int J Hydrogen Energy 2008;33:7513–20.
[15] Park H. Effect of the hydrophilic and hydrophobic characteristics of the gas diffusion medium on polymer electrolyte fuel cell performance under non-humidification condition. Energy Convers Manage 2014;81:220–30.
[16] Cha D, Ahn JH, Kim HS, Kim Y. Effects of clamping force on the water transport and performance of a PEM (proton electrolyte membrane) fuel cell with relative humidity and current density. Energy 2015;93:1338–44.
[17] Dai W, Wang H, Yuan XZ, Martin JJ, Yang D, Qiao J, et al. A review on water balance in the membrane electrode assembly of proton exchange membrane fuel cells. Int J Hydrogen Energy 2009;34:9461–78.
[18] Li J, Li X, Yu S, Hao J, Lu W, Shao Z, et al. Porous polybenzimidazole membranes doped with phosphoric acid: preparation and application in high-temperature proton-exchange-membrane fuel cells. Energy Convers Manage 2014;85:323–7.
[19] Liso V, Araya SS, Olesen AC, Nielsen MP, Kær SK. Modeling and experimental validation of water mass balance in a PEM fuel cell stack. Int J Hydrogen Energy 2016;41:3079–92.
[20] Saeed F, Saidan M, Said A, Mustafa M, Abdelhadi A, Al-Weissi S. Effect of flow rate, flow direction, and silica addition on the performance of membrane and the corrosion behavior of Pt–Ru/C catalyst in PEMFC. Energy Convers Manage 2013;75:36–43.
[21] Das PK, Li X, Liu ZS. Analysis of liquid water transport in cathode catalyst layer of PEM fuel cells. Int J Hydrogen Energy 2010;35:2403–16.
[22] Hsieh SS, Her BS, Huang YJ. Effect of pressure drop in different flow fields on water accumulation and current distribution for a micro PEM fuel cell. Energy Convers Manage 2011;52:975–82.
[23] Bao C, Bessler WG. Two-dimensional modeling of a polymer electrolyte membrane fuel cell with long flow channel. Part I. Model development. J Power Sources 2015;275:922–34.
[24] Mahmoudi A, Ramiar A, Esmaili Q. Effect of inhomogeneous compression of gas diffusion layer on the performance of PEMFC with interdigitated flow field. Energy Convers Manage 2016;110:78–89.
[25] Jeon DH, Kim KN, Baek SM, Nam JH. The effect of relative humidity of the cathode on the performance and the uniformity of PEM fuel cells. Int J Hydrogen Energy 2011;36:12499–511.
[26] Misran E, Hassan NSM, Daud WRW, Majlan EH, Rosli MI. Water transport characteristics of a PEM fuel cell at various operating pressures and temperatures. Int J Hydrogen Energy 2013;38:9401–8.
[27] Tang H, Wang S, Jiang SP, Pan M. A comparative study of CCM and hot-pressed MEAs for PEM fuel cells. J Power Sources 2007;170:140–4.
[28] Li Q, Xiao C, Zhang H, Chen F, Fang P, Pan M. Polymer electrolyte membranes containing titanate nanotubes for elevated temperature fuel cells under low relative humidity. J Power Sources 2011;196:8250–6.
[29] Tu Z, Zhang H, Luo Z, Liu J, Wan Z, Pan M. Evaluation of 5 kW proton exchange membrane fuel cell stack operated at 95 °C under ambient pressure. J Power Sources 2013;222:277–81.
[30] Altria KD. Additional application areas of capillary electrophoresis. In: Capillary electrophoresis guidebook: principles, operation and applications. New Jersey: Humana Press Inc.; 1996. p. 309–44 [chapter 20].
[31] Yang RJ, Fu LM, Lin YC. Electroosmotic flow in microchannels. J Colloid Interface Sci 2001;239:98–105.
[32] Doherty EA, Meagher RJ, Albarghouthi MN, Barron AE. Microchannel wall coatings for protein separations by capillary and chip electrophoresis. Electrophoresis 2003;24:34–54.
[33] Dolník V. Wall coating for capillary electrophoresis on microchips. Electrophoresis 2004;25:3589–601.
[34] Nguyen TV, White RE. A water and heat management model for proton-exchange-membrane fuel cells. J Electrochem Soc 1993;140:2178–86.